

To be submitted to Eur. Phys. J. C

# Study of $K^+ \rightarrow \pi^0 e^+ \nu \gamma$ decay with OKA setup

A.Yu. Polyarush<sup>a</sup>, V.A. Duk<sup>b</sup>, S.N. Filippov, E.N. Guschin, A.A. Khudiyakov, V.I. Kravtsov,  
Yu.G. Kudenko<sup>cd</sup>,

(INR RAS, MOSCOW, RUSSIA),

S.A. Akimenko, A.V. Artamonov, A.M. Blik, V.S. Burtovoy, S.V. Donskov, A.P. Filin, A.V. Inyakin,

A.M. Gorin, G.V. Khaustov, S.A. Kholodenko, V.N. Kolosov, V.F. Kurshetsov, V.A. Lishin,

M.V. Medynsky, Yu.V. Mikhailov, V.F. Obraztsov, V.A. Polyakov, V.I. Romanovsky, V.I. Rykalin,

A.S. Sadovsky, V.D. Samoilenko, M.M. Shapkin, O.V. Stenyakin, O.G. Tchikilev, V.A. Uvarov,

O.P. Yushchenko

(NRC "KURCHATOV INSTITUTE" - IHEP, PROTVINO, RUSSIA),

V.N. Bychkov, G.D. Kekelidze, V.M. Lysan, B.Zh. Zalikhanov

(JINR, DUBNA, RUSSIA)

<sup>a</sup>e-mail: polyarush@inr.ru

<sup>b</sup>Now at INFN-Sezione di Perugia, Via A. Pascoli, 06123 Perugia, Italy

<sup>c</sup>Also at Moscow Institute of Physics and Technology, Moscow, Russia

<sup>d</sup>Also at NRNU Moscow Engineering Physics Institute (MEPhI), Moscow, Russia

## Abstract

Results of a study of the  $K^+ \rightarrow \pi^0 e^+ \nu \gamma$  decay at OKA setup are presented. More than 32000 events of this decay are observed. The differential spectra over the photon energy and the photon-electron opening angle in kaon rest frame are presented. The branching ratios, normalized to that of  $K_{e3}$  decay are calculated for different cuts in  $E_\gamma^*$  and  $\cos\Theta_{e\gamma}^*$ . In particular, the branching ratio for  $E_\gamma^* > 30$  MeV and  $\Theta_{e\gamma}^* > 20^\circ$  is measured  $R = \frac{Br(K^+ \rightarrow \pi^0 e^+ \nu \gamma)}{Br(K^+ \rightarrow \pi^0 e^+ \nu)}$   $= (0.587 \pm 0.010(stat.) \pm 0.015(syst.)) \times 10^{-2}$ , which is in a good agreement with ChPT  $O(p^4)$  calculations.

## 1 Introduction

The decay  $K^+ \rightarrow \pi^0 e^+ \nu \gamma$  provides fertile testing ground for the Chiral Perturbation Theory (ChPT) [1, 2], the effective field theory of the Standard Model at low energies.

$K^+ \rightarrow \pi^0 e^+ \nu \gamma$  decay was first considered in [3] up to the order ChPT  $O(p^4)$  and branching ratios were evaluated for given cuts in the photon energy and in the photon-electron opening angle in the kaon rest frame:  $E_\gamma^* > E_\gamma^{cut}$ ,  $\Theta_{e\gamma}^* > \Theta_{e\gamma}^{cut}$ . Later the CHPT analysis was revisited and extended to  $O(p^6)$  [4]. The branchings at tree level were also calculated in papers [5, 6], as well as T-odd correlations.

The matrix element for  $K^+ \rightarrow \pi^0 e^+ \nu \gamma$  decay has general structure

$$T = \frac{G_F}{\sqrt{2}} e V_{us} \varepsilon^\mu(q) \left\{ (V_{\mu\nu} - A_{\mu\nu}) \bar{u}(p_\nu) \gamma^\nu (1 - \gamma_5) v(p_e) + \frac{F_V}{2p_{e\gamma}} \bar{u}(p_\nu) \gamma^\nu (1 - \gamma_5) (m_e - \hat{p}_e - \hat{q}) \gamma_\mu v(p_e) \right\} \equiv \varepsilon^\mu A_\mu.$$

First term of the matrix element describes the bremsstrahlung of kaon and the direct emission. The relevant diagram is displayed in Fig.1a. The lepton bremsstrahlung is presented by the second part of Eq.(1) and Fig.1b. The hadronic tensors  $V_{\mu\nu}^{had}$  and  $A_{\mu\nu}^{had}$  are defined by  $I_{\mu\nu} = i \int d^4 e^{iqx} \langle \pi^0(p') | T V_\mu^{em}(x) I_\nu^{had}(0) | K^+(p) \rangle$ ,  $I = V, A$ , with  $V_\nu^{had} = \bar{s} \gamma_\nu u$ ,  $A_\nu^{had} = \bar{s} \gamma_\nu \gamma_5 u$ ,  $V_\mu^{em} = (2\bar{u} \gamma_\mu u - \bar{d} \gamma_\mu d - \bar{s} \gamma_\mu s)/3$  and  $F_V$  is the  $K_{e3}^+$  matrix element  $F_V = \langle \pi^0(p') | V_\nu^{had}(0) | K^+(p) \rangle$ .

The bremsstrahlung part of the amplitude is largely dominant in the partial decay width. Only with the advent of high statistics kaon decay experiments it become feasible to study effects of structure dependent contributions and of the chiral anomaly.

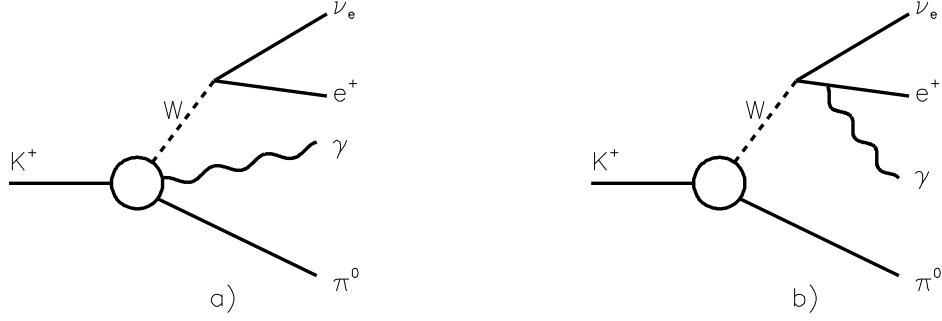


Figure 1: Diagrams describing  $K^+ \rightarrow \pi^0 e^+ \nu \gamma$  decay

The numerical results given in [3–6] demonstrate that non-trivial CHPT effects can be detected by the experiment. This gives a motivation for the present study.

## 2 OKA setup

OKA collaboration operates at IHEP Protvino U-70 Proton Synchrotron. OKA detector (see Fig.2) is located in positive RF-separated beam with 12.5% of kaon with a momentum of 17.7 GeV/c and an intensity of  $3 \cdot 10^5$  kaons per 2 sec U-70 spill. RF-separation with the Panofsky scheme is realized. It uses two superconductive

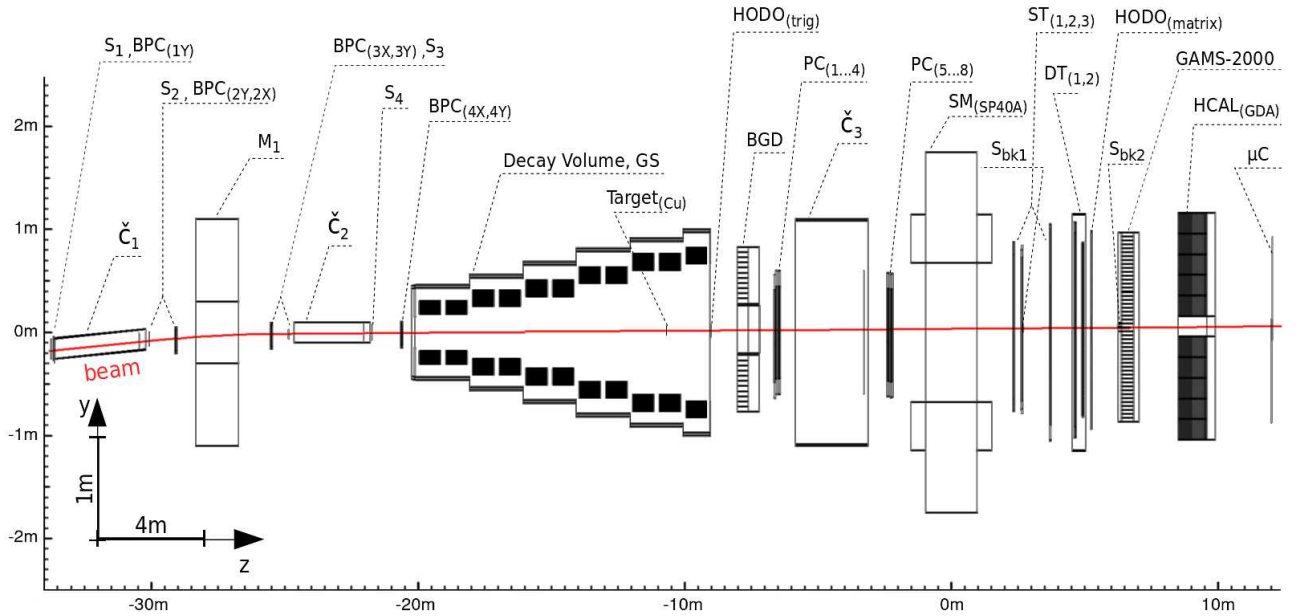


Figure 2: Layout of the OKA detector

Karlsruhe-CERN SC RF deflectors[7], donated by CERN. Sophisticated cryogenic system, built at IHEP[8]

provides superfluid He for cavities cooling. The detailed description of the OKA detector is given in our previous publications [9, 10]. The OKA is taking data since 2010. In this study, we use the statistics that was obtained in the 2012 and 2013 years. The total number of kaons entering the Decay volume (DV) corresponds to  $\sim 3.4 \times 10^{10}$ .

Rather simple trigger was used during data-taking:  $\text{Tr} = S_1 \cdot S_2 \cdot S_3 \cdot S_4 \cdot \bar{C}_1 \cdot \check{C}_2 \cdot \bar{S}_{bk} \cdot (E_{GAMS} > 2.5 \text{ GeV})$ .  $S_1 - S_4$  are scintillating counters;  $\check{C}_1, \check{C}_2$  - Cherenkov counters ( $\check{C}_1$  sees pions,  $\check{C}_2$  pions and kaons);  $S_{bk}$  - two scintillation counters on the beam axis after the magnet to suppress undecayed particles.

The MC simulation of the OKA setup is done within the GEANT3 framework[11]. Signal and background events are weighted according to corresponding matrix elements.

### 3 Events selection and background suppression

Criteria for events selection:

- 1) One positive charged track detected in the tracking system and 4 showers detected in the electromagnetic calorimeters GAMS- 2000 and BGD.
- 2) One shower must be associated with the charged track.
- 3) The charged track is identified as a positron. The positron identification is done using the ratio of the energy of the shower in GAMS- 2000 to the momentum of the associated track. The  $E/p$  distribution is shown in Fig.3. The particles with  $0.8 < E/p < 1.2$  are accepted as positrons. Another cut used for the suppression of the  $\pi^+$  contamination is that on the distance between the charged track extrapolation to the front plane of the electromagnetic detector and the nearest shower. This distance must be less than 3 cm.

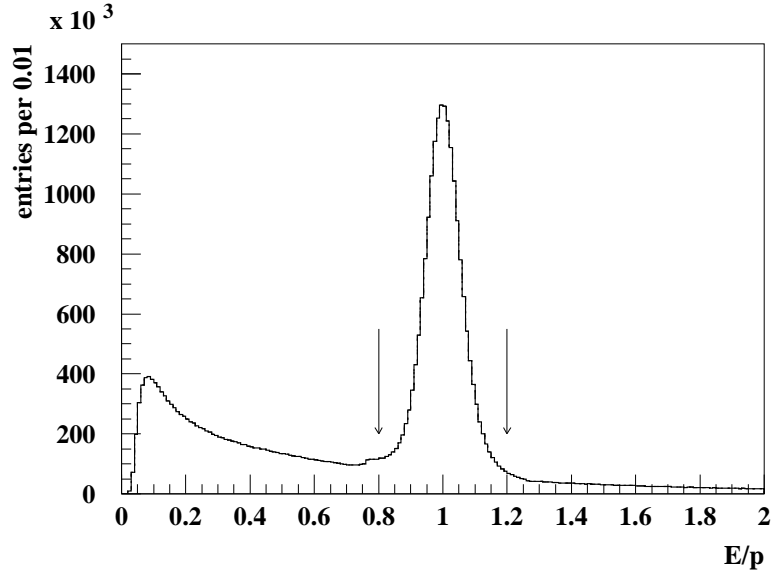


Figure 3:  $E/p$  ratio for the real data.

- 4) The decay vertex situated within the decay volume.
- 5) The mass  $M_{\gamma\gamma}$  of the  $\gamma\gamma$  - pair closest to the Table value of  $\pi^0$  is  $0.12 < M_{\gamma\gamma} < 0.15 \text{ GeV}$ . Energy of a photon originated from  $\pi^0$  is greater than 0.5 GeV. Energy of the radiative photon is greater than 0.8 GeV. Absence of signals in veto system above noise threshold is also required.

The main background decay channels for the decay  $K^+ \rightarrow \pi^0 e^+ \nu_e \gamma$  are:

- 1)  $K^+ \rightarrow \pi^0 e^+ \nu$  with an extra photon. The main source of extra photons is the positron interactions in the detector.

- 2)  $K^+ \rightarrow \pi^+ \pi^0 \pi^0$  where one of the  $\pi^0$  photons is not detected and  $\pi^+$  is misidentified as a positron.
- 3)  $K^+ \rightarrow \pi^+ \pi^0$  with a “fake photon” and  $\pi^+$  miss-identified as a positron. The fake photon clusters can come from  $\pi n$  interaction in the gamma detector, and from accidentals.
- 4)  $K^+ \rightarrow \pi^+ \pi^0 \gamma$  when  $\pi^+$  is miss-identified as a positron.
- 5)  $K^+ \rightarrow \pi^0 \pi^0 e^+ \nu$  when one  $\gamma$  is lost.

All these background sources are included in our MC calculations.

To suppress the background channels we use a set of cuts:

Cut 1:  $E_{miss} > 0.5$  GeV. The requirement on the missing energy mainly reduces background (4).

Cut 2:  $\Delta y = |y_\gamma - y_e| > 5$  cm, where  $y$  is the vertical coordinate of a particle in the electromagnetic calorimeter. (the magnetic field turns charged particles in xz-plane).

Cut 3:  $|x_v, y_v| < 100$  cm. The reconstructed missing momentum direction must cross the active area of the electromagnetic calorimeter.

Cut 4:  $M_{K \rightarrow \pi^0 e^+ \nu_e \gamma} > 0.45$  GeV.  $M_{K \rightarrow \pi^0 e^+ \nu_e \gamma}$  - the reconstructed mass of the  $(\pi^0 e^+ \nu_e \gamma)$ - system, assuming  $m_\nu = 0$ . To enforce this cut we use a cut on the missing mass squared  $M^2(\pi^0 e \gamma) = (P_K - P_{\pi^0} - P_e - P_\gamma)^2$ . For the signal events this variable corresponds to the square of the neutrino mass and must be zero within measurement accuracy.

Cut 5:  $-0.003 < M^2(\pi^0 e^+ \gamma) < 0.003$ . The dominant background to  $K_{e3\gamma}$  arises from  $K_{e3}$  with an extra photon (background (1)). This background is suppressed by a requirement on the angle between positron and photon in the laboratory frame  $\Theta_{e\gamma}$  (see Fig.4). The distribution of the  $K_{e3}$ -background events has a very sharp peak at zero angle. This peak is significantly narrower than that for the signal events. This happens, in particular, because the emission of the photons by the positron occurs in the setup material downstream the decay vertex, but the angle is still calculated as if emission comes from the vertex.

Cut 6:  $0.004 < \Theta_{e\gamma} < 0.080$ . Left part of this cut is introduced exactly for the suppression of background (1). The right cut is against  $K_{\pi 2}$  background.

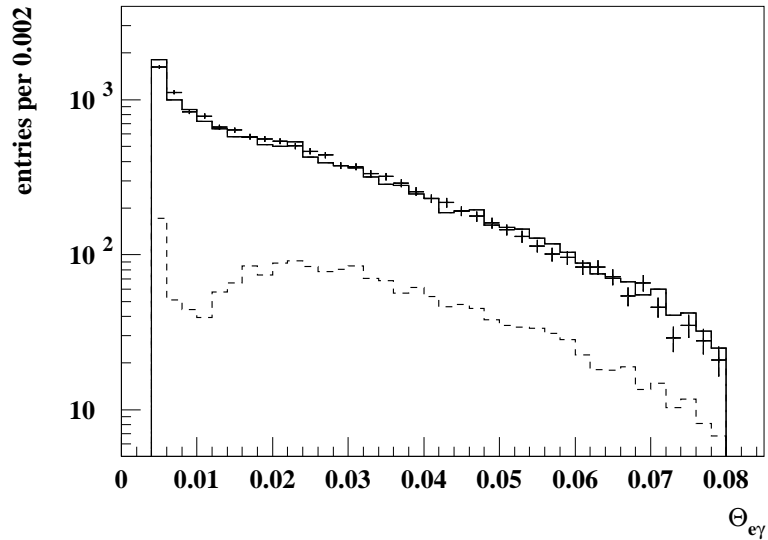


Figure 4: Distribution over  $\Theta_{e\gamma}$  - the angle between positron and photon in lab. system. Real data (points with errors), signal plus MC background (solid line histogram), MC background (dotted line histogram).

After all the cuts, 32676 candidates are selected, with a background of 4624 events. Background normalization is done by comparison of the number of events for  $K_{e3}$  decay in MC and real data samples.

## 4 Results

The resulting distribution of the selected events over  $\cos(\Theta_{e\gamma}^*)$ ,  $\Theta_{e\gamma}^*$  being the angle between the positron and the photon in the kaon rest frame, is shown in Fig.5.

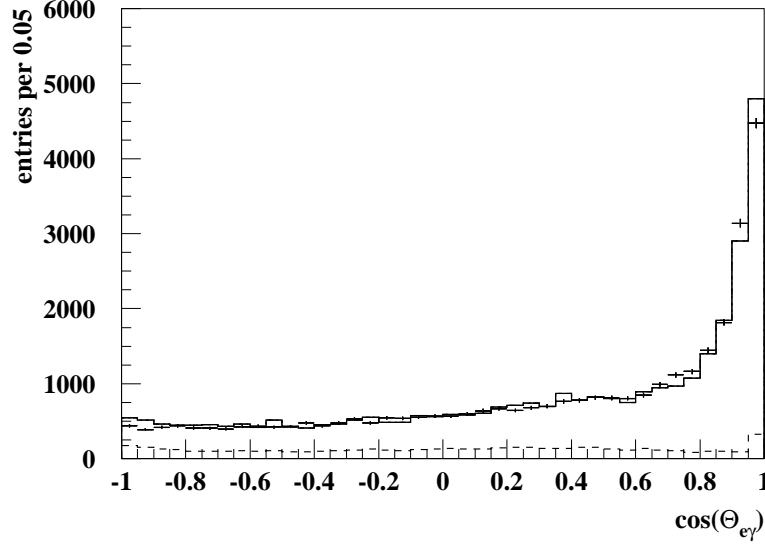


Figure 5: The distribution of the events over  $\cos\Theta_{e\gamma}^*$ . Points with errors - the real data, histogram - MC signal plus background, MC background - dotted line histogram.

The distribution over  $E_{e\gamma}^*$  - the photon energy in the kaon rest frame is shown in Fig.6. Reasonable agreement of the data with MC is seen. When generating the signal MC, a generator based on  $O(p^4)$  calculations[3] is used.

To obtain the branching ratio for the  $K_{\pi^0 e^+ \nu_e \gamma}$  relative to the  $K_{e3}$  (R), the background and efficiency corrected number of  $K_{e3\gamma}$  events is normalized on that of about 9M  $K_{e3}$  events found with a similar selection criteria.

The relative branching ratio (R) for the soft cuts  $E_{\gamma}^* > 10$  MeV and  $\Theta_{e\gamma}^* > 10^\circ$  is found to be

$$R_1 = \frac{Br(K^+ \rightarrow \pi^0 e^+ \nu_e \gamma)}{Br(K^+ \rightarrow \pi^0 e^+ \nu_e)} = (1.990 \pm 0.017(stat.) \pm 0.021(syst.)) \times 10^{-2}.$$

And for the cuts  $E_{\gamma}^* > 30$  MeV and  $\Theta_{e\gamma}^* > 20^\circ$  used for the comparison with theory we have

$$R_2 = \frac{Br(K^+ \rightarrow \pi^0 e^+ \nu_e \gamma)}{Br(K^+ \rightarrow \pi^0 e^+ \nu_e)} = (0.587 \pm 0.010(stat.) \pm 0.015(syst.)) \times 10^{-2}.$$

For the comparison with previous experiments the branching ratio with the cuts  $E_{\gamma}^* > 10$  MeV,  $0.6 < \cos\Theta_{e\gamma}^* < 0.9$  is calculated

$$R_3 = \frac{Br(K^+ \rightarrow \pi^0 e^+ \nu_e \gamma)}{Br(K^+ \rightarrow \pi^0 e^+ \nu_e)} = (0.532 \pm 0.010(stat.) \pm 0.012(syst.)) \times 10^{-2}.$$

Systematic errors are estimated by variation of the cuts 1-6. Contributions of each cut variation to systematic errors are given in Table 1.

The comparison with previous experiments is given in Table 2.

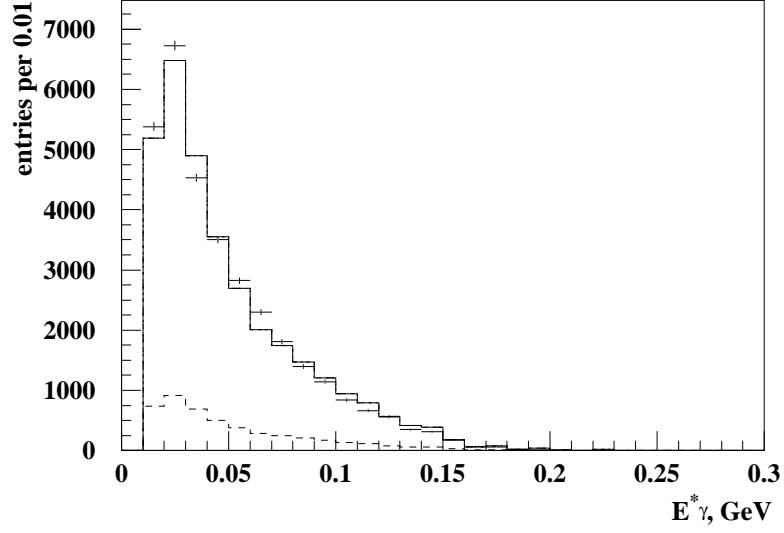


Figure 6: The distribution of the events over  $E_{e\gamma}^*$ . Points with errors is the real data, histogram - MC signal plus background, MC background - dotted line histogram.

Table 1: Contributions to systematic errors.

| $R_i$ | 1     | 2     | 3     | 4     | 5     | 6     |
|-------|-------|-------|-------|-------|-------|-------|
| $R_1$ | 0.003 | 0.002 | 0.006 | 0.008 | 0.015 | 0.011 |
| $R_2$ | 0.004 | 0.001 | 0.004 | 0.005 | 0.010 | 0.008 |
| $R_3$ | 0.001 | 0.001 | 0.005 | 0.001 | 0.010 | 0.004 |

Table 2:  $\text{Br}(K^+ \rightarrow \pi^0 e^+ \nu_e \gamma) / \text{Br}(K^+ \rightarrow \pi^0 e^+ \nu_e)$  for  $E_\gamma^* > 10$  MeV,  $0.6 < \cos\Theta_{e\gamma}^* < 0.9$  in comparison with previous data.

| $R_3 \times 10^2$        | $N_{ev}$ | experiment      |
|--------------------------|----------|-----------------|
| $0.53 \pm 0.01 \pm 0.01$ | 7248     | this experiment |
| $0.48 \pm 0.02 \pm 0.03$ | 1423     | ISTRA+ [12]     |
| $0.46 \pm 0.08$          | 82       | XEBC [13]       |
| $0.56 \pm 0.04$          | 192      | ISTRA [14]      |
| $0.76 \pm 0.28$          | 13       | HLBC [15]       |

## Conclusions

The largest statistics of about 32K events of  $K_{e3\gamma}$  is collected by the OKA experiment. The relative branching ratio  $R = \text{Br}(K^+ \rightarrow \pi^0 e^+ \nu_e \gamma) / \text{Br}(K^+ \rightarrow \pi^0 e^+ \nu_e)$  is measured for different cuts on the photon energy and the photon-electron angle in the kaon rest frame. The obtained value of  $R$  for  $E_\gamma^* > 30$  MeV and  $\Theta_{e\gamma}^* > 20^\circ$  is in a good agreement with the CHPT  $O(p^4)$  prediction[3]  $R = (0.592 \pm 0.005) \times 10^{-2}$  and is some  $2\text{--}3\sigma$  away from the tree level results[5, 6]. The  $O(p^6)$  result[4] is  $2.5\sigma$  higher. That is, the measurement becomes sensitive to the non-trivial CHPT effects.

## Acknowledgements

The authors express their gratitude to the colleagues from the accelerator Department for good performance of the U-70 during data taking; to colleagues from the beam department for the stable operation of the 21K beam line, including RF-deflectors, and to colleagues from the engineering physics department for the operation of the cryogenic system of the RF-deflectors.

The work is supported in part by the Russian Fund for Basic Research, grant N18-02-00179A.

## References

- [1] S.Weinberg, *Physica A* **96**, 327 (1979)
- [2] J.Gasser and H.Leutwyler, *Nucl. Phys. B* **250**, 465 (1985)
- [3] J. Bijnens, G. Echer and J. Gasser, *Nucl. Phys. B* **396**, 81 (1993)
- [4] B.Kubis *et al.*, *Eur Phys. J. C* **50**, 557(2007)
- [5] V. V. Braguta, A. A. Likhoded, A. E. Chalov, *Phys. Rev. D* **65**, 054038 (2002)
- [6] I.B. Khriplovich, A.S. Rudenko, *Phys. Atom. Nucl.* **74**, 1214 (2011)
- [7] A. Citron *et al.*, *Nucl. Instrum. Methods Phys. Res.* **164**, 31 (1979)
- [8] 3. A. Ageev *et al.* in Proceedings of the Russian Particle Accelerator Conference RuPAC, Zvenigorod, Russia, 2008, p. 282
- [9] A.S. Sadovsky *et al.*, *Eur. Phys. J. C* **78**, 92 (2018), arXiv:1709.01473 [hep-ex]
- [10] M.M. Shapkin *et al.*, *Eur. Phys. J. C* **79**, 296 (2019), arXiv:1808.09176 [hep-ex]
- [11] R. Brun *et al.* CERN-DD/EE/84-1.
- [12] V.N.Bolotov *et al.*, *Yad. Fiz.* **70**, 1 (2007), *Phys. Atom. Nucl.* **70**, 29 (2007)
- [13] V.V.Barmin *et al.*, *SJNP* **53**, 606 (1991), *Yad. Fiz.* **53**, 981 (1991)
- [14] V.N.Bolotov *et al.*, *JETP Lett.* **42**, 68 (1986), *Yad. Fiz.* **44**, 108 (1986), *Sov.J.Nucl.Phys.* **44**, 68 (1986)
- [15] F.Romano *et al.*, *Phys Lett. B* **36**, 525 (1971)